Control of magnetism by crystal chemistry in T'-phase $R_2Cu_{1-x}Pd_xO_4$ (R=Nd, Sm, Eu, Gd; $0 \leqslant x \leqslant 0.2$)

J. F. Vente and P. D. Battle*
Inorganic Chemistry Laboratory, University of Oxford, South Parks Road, Oxford, OX1 3QR, United Kingdom
(Received 23 December 1997)

Polycrystalline samples of the T'-phases $R_2Cu_{1-x}Pd_xO_4$ (R=Nd, Sm, Eu, Gd; $0 \leqslant x \leqslant 0.2$) have been characterized by x-ray powder diffraction (XRPD) and magnetometry. Doping with diamagnetic Pd induces orthorhombic symmetry and hence weak ferromagnetism in the Sm ($x \geqslant 0.1$) and Eu ($x \geqslant 0.05$) phases, which are antiferromagnetic for $x=0.0$. The structural distortion is too subtle to be observed directly by XRPD, but it is shown that the derivative $\partial(c/a)/\partial x$ (positive for orthorhombic, ferromagnetic phases and negative for the tetragonal phases) can be used as a diagnostic. The dopant concentration necessary to induce the transition is determined by the ratio of ionic radii r_R/r_M, where r_M is the mean radius of the four coordinate cation (Pd/Cu). Samples having $r_R/r_M < 1.87$ are weak ferromagnets; Nd^{3+} is too large for this condition to be satisfied in the composition range studied, whereas Gd^{3+} is too small to stabilize tetragonal T'-phases. There is evidence for re-entrant spin-glass behavior in Pd-free Eu_2CuO_4. [S0163-1829(98)06929-X]

INTRODUCTION

The magnetic properties of layered copper oxides have been studied in great detail since the discovery of high-T_c superconductivity in K_2NiF_4-like $La_{2-x}Ba_xCuO_4$.[1] Interest in the so-called T' compounds[2] R_2CuO_4 (R=Pr, Nd, Sm, and Eu) grew when it was discovered that Ce-doped samples become superconducting at $\sim$24 K.[3,4] In contrast to $La_{2-x}A_xCuO_4$ (A=Sr, Ba), the conductivity in the doped T'-phases is n type rather than p type. The observation of superconductivity in the Ce-containing samples prompted a number of investigations into the magnetic properties of the undoped parent compounds R_2CuO_4. The research carried out to date on these oxides has shown that the details of the behavior involving the R cation are very sensitive to the chemical composition of the sample, whereas the Cu sublattice always appears to show long-range magnetic order below $\sim$270 K.[5] Nd_2CuO_4 has an undistorted T' structure[2] (space group $I4/mmm$), built up from xy sheets of vertex-sharing Cu-O squares (Fig. 1) which are separated along z by R_2O_2 layers in which the R^{3+} and O^{2-} ions are eight coordinate and four coordinate, respectively. The most striking difference between this structure and that of the T phases (e.g., K_2NiF_4, La_2CuO_4) is the reduction in the coordination number of Cu from 6 to 4. The magnetic interactions involving the Cu sublattice in Nd_2CuO_4 have a strong two-dimensional (2D) character, but 3D long-range antiferromagnetic order is achieved at $T_N \sim 260$ K despite the fact that the interlayer interactions are frustrated. A small magnetic moment is induced on the Nd cations at all temperatures below T_N, and it has been suggested that their involvement nullifies the magnetic frustration on the Cu^{2+} sublattice, although the details of the argument are not clear.[6–10] Immediately below T_N the magnetic structure is the same as that found in La_2NiO_4 (Ref. 11) and Pr_2CuO_4,[9] but in the temperature range $30 < T/K < 75$ a magnetic structure similar to that of La_2CuO_4 (Ref. 12) is adopted. However, variations in the relative strengths of the different intercation interactions cause the spins to revert to their high-temperature arrangement for $T < 30$ K. The Nd sublattice finally achieves antiferromagnetic order at 1.7 K.[9,13,14] The behavior of Sm_2CuO_4 is somewhat different from that of Nd_2CuO_4. Although long-range ordering of the Cu sublattice occurs at approximately the same temperature, there is no high-temperature coupling between the Cu^{2+} and Sm^{3+} spins.[15,16] At all temperatures $6 < T/K < T_N$ Sm_2CuO_4 adopts the magnetic structure of La_2CuO_4 and the Sm spins eventually order antiferromagnetically at 5.95 K.[17] The behavior of Eu_2CuO_4 is similar to that of the Sm analog, with the Cu-sublattice ordering at approximately the same temperature and with the same magnetic structure.[18–20] No magnetic ordering on the lanthanide sublattice is observed due to the nonmagnetic ground state of Eu^{3+}. The reasons for the differences in the behavior of the Cu sublattice as the nature of R changes are not fully understood, but the apparent dependence of the magnetic properties on the R cation becomes even more marked when the compound Gd_2CuO_4 is also considered. The Cu sublattice in this compound has been reported to order at $\sim$260 K,[21] but the ordered phase is a weak ferromagnet rather than an antiferromagnet. The canting of the Cu spins is inconsistent with

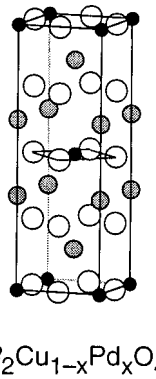

FIG. 1. T' crystal structure of $R_2Cu_{1-x}Pd_xO_4$. Large shaded circles represent R ions, small black circles Cu ions, and large open circles oxide ions.

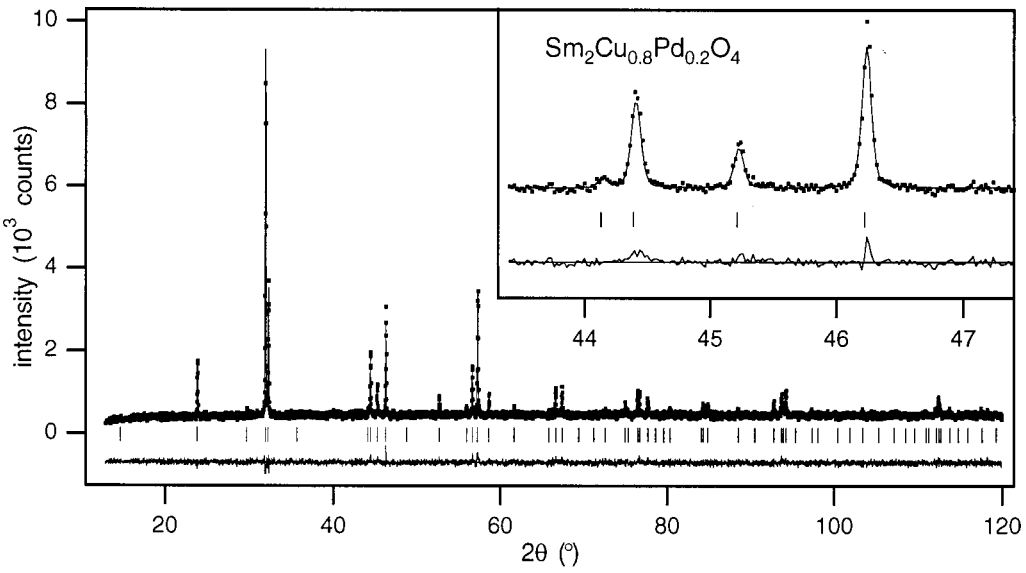

FIG. 2. Observed, calculated, and difference room-temperature x-ray-diffraction patterns for $Sm_2Cu_{0.8}Pd_{0.2}O_4$. Reflection positions are marked. The inset shows the {1 1 4}, {1 0 5}, {0 0 6}, and {2 0 0} reflections.

the symmetry elements of space group $I4/mmm$, and it has been established that, at temperatures below 658(1) K, the unit cell is enlarged to $\sim a\sqrt{2}\times\sim a\sqrt{2}\times c$, and the space-group symmetry is reduced to *Acam*.[22,23] The principal structural change is a 5.2° rotation of the CuO_4 squares around the z axis. As a result of the reduction of the symmetry from tetragonal to orthorhombic, the interlayer Cu-Cu coupling is no longer frustrated. The Gd sublattice is antiferromagnetically ordered below 6.5 K,[21] and it has been suggested that Gd-Gd interactions become competitive with Cu-Gd and Cu-Cu interactions at ~20 K. The experimental evidence for this proposal[21] is the observation of a susceptibility maximum at a temperature which decreases with increasing applied field, and only corresponds to the ordering temperature of the Gd sublattice in the high-field limit. Further evidence for the existence of the Cu-Gd interactions has been provided by a numerical analysis of the in-plane magnetization anisotropy in Gd_2CuO_4 single crystals.[24] Studies of high-pressure T'-phases containing the smaller lanthanides (Tb, Dy, Ho, Er, Tm, and Y) (Ref. 25) have also revealed evidence of weak ferromagnetism, and an additional spin-glass component was identified in the susceptibility. Many attempts have been made to elucidate the behavior of this family of compounds using a wide variety of experimental techniques. One strategy[26,27] has been to prepare mixed lanthanide compounds, for example $Sm_{2-y}Gd_yCuO_4$, and to monitor the magnetic properties as a function of composition. The results of these experiments[27] have been interpreted in terms of the size of the crystal lattice, with the suggestion that the existence of weak ferromagnetism may be associated with a misfit of the R_2O_2 layers and the CuO_2 sheets when the ionic radius of the R cation becomes too small. We describe below a series of experiments designed to study this effect in a different way, that is by substituting relatively small concentrations of Pd onto the Cu sublattice. Pd^{2+} has a strong preference for square-planar coordination and the structural chemistry of the T'-phase is therefore compatible with this doping. The Pd^{2+} cation has a $4d^8$ electron configuration and is expected to be diamagnetic in the T' structure. It is larger than Cu^{2+},[28] and we are therefore replacing an $S=1/2$ cation with a larger $S=0$ cation. If the relative size of the R and Cu sublattices is an important factor in determining the magnetic properties of the T' R_2CuO_4 compounds, then it might be expected that Pd doping will induce weak ferromagnetism in compounds containing R cations larger than Gd^{3+}, provided that the degree of dilution of the Cu sublattice is not too great.

EXPERIMENT

Polycrystalline samples $R_2Cu_{1-x}Pd_xO_4$ (R=Nd, Sm, Eu, Gd; $0\leqslant x\leqslant 0.2$) were prepared by firing stoichiometric, pelletized mixtures of dry R_2O_3, CuO, and PdO (all Johnson Matthey Chemicals) in alumina crucibles. Reactions were started at a temperature of 700 °C, increasing in steps of 25 °C every two days in order to prevent the loss of Pd. The maximum temperature was in all cases between 950 and 975 °C. X-ray data (Cu $K\alpha_1$) were recorded using a Siemens D5000 diffractometer operating at room temperature in Bragg-Brentano geometry over the angular range $5\leqslant 2\theta/^\circ \leqslant 120$, with a step size of 0.02°. The results of our powder diffraction experiments were analyzed by the Rietveld method[29] using the GSAS program package.[30] The peak shape was described by a pseudo-Voigt function and the background level was fitted with a shifted Chebyshev function. For each diffraction pattern, a scale factor, a counter zeropoint, four peak-shape parameters, ten background parameters, two unit-cell parameters, one fractional coordinate, and four isotropic thermal parameters were refined.

Magnetization measurements were performed on a Quantum Design MPMS superconducting quantum interference device magnetometer in the temperature range $5\leqslant T/\mathrm{K} \leqslant 300$ in magnetic fields of 10, 100 G, and 1 kG. All measurements were taken on warming from the lowest temperature after both zero-field cooling (ZFC) and cooling in the measuring field (FC). Zero-field-cooled and field-cooled

TABLE I. Room-temperature unit-cell parameters of $R_2Cu_{1-x}Pd_xO_4$ with R=Nd, Sm, Eu, and Gd; $0 \leqslant x \leqslant 0.2$. r_M is the concentration-weighted mean radius of the four-coordinate cation.

x	r_R/r_M	a (Å)	c (Å)	V (Å^3)
$Nd_2Cu_{1-x}Pd_xO_4$				
0.00	1.946	3.943 20(3)	12.1712(1)	189.249(3)
0.05	1.934	3.945 81(6)	12.1748(2)	189.569(7)
0.10	1.922	3.948 60(7)	12.1783(3)	189.878(9)
0.15	1.910	3.951 66(8)	12.1835(4)	190.25(1)
0.20	1.899	3.954 63(9)	12.1889(4)	190.63(1)
$Sm_2Cu_{1-x}Pd_xO_4$				
0.00	1.893	3.915 27(8)	11.9766(3)	183.59(1)
0.025	1.887	3.916 63(5)	11.9789(2)	183.756(7)
0.05	1.881	3.917 12(6)	11.9793(2)	183.809(8)
0.075	1.876	3.919 22(8)	11.9855(3)	184.10(1)
0.10	1.870	3.922 54(8)	11.9948(3)	184.56(1)
0.15	1.859	3.925 06(9)	12.0161(4)	185.12(1)
0.20	1.848	3.928 17(7)	12.0344(3)	185.698(9)
$Eu_2Cu_{1-x}Pd_xO_4$				
0.00	1.870	3.902 78(5)	11.9071(2)	181.365(6)
0.05	1.859	3.905 71(8)	11.9235(3)	181.89(1)
0.10	1.847	3.909 47(6)	11.9494(3)	182.634(8)
0.15	1.836	3.913 42(8)	11.9729(3)	183.36(1)
0.20	1.825	3.917 23(9)	11.9965(4)	184.08(1)
$Gd_2Cu_{1-x}Pd_xO_4$				
0.00	1.847	3.896 54(5)	11.8914(2)	180.548(7)
0.05	1.836	3.899 28(8)	11.9106(4)	181.09(1)
0.10	1.825	3.903 2(2)	11.9294(5)	181.74(2)
0.15	1.814	3.906 1(1)	11.9456(4)	182.26(1)
0.20	1.803	3.909 2(2)	11.9605(8)	182.78(3)

(cooled in 2 kG) hysteresis loops in the range $-2 \leqslant H/\text{kG} \leqslant 2$ were recorded for selected compounds and, where appropriate, FC magnetization measurements were made over larger temperature ranges and in larger magnetic fields. We estimate that the uncertainty in the applied magnetic fields is about 5 G for $H \geqslant 100$ G and about 1 G for $H = 10$ G.

RESULTS

We prepared samples with the general formula $R_2Cu_{1-x}Pd_xO_4$ [R=Nd, Sm, Eu, Gd; x=0, 0.025 (Sm only), 0.05, 0.075 (Sm only), 0.10, 0.15, 0.20]. Some of the samples prepared (i.e., R=Nd: x=0.05, 0.15, and R=Sm; x=0.025) were used only to provide additional data for our study of the composition dependence of the unit-cell parameters; they were not investigated by magnetometry. The Pd content of selected samples was determined by inductively coupled plasma atomic emission analysis and was always found to be in agreement with the nominal value.

Crystallographic characterization

The refinements of the structures of all compounds under investigation proceeded smoothly in the space group $I4/mmm$. Our compounds were modeled using a random distribution of Cu and Pd, since no indication of a possible ordering between Cu and Pd was observed. The final agreement indices were in all cases low: $\chi^2_{\text{red}} \leqslant 1.2$; $5.5 \leqslant R_{wp}/\% \leqslant 9$. The observed and calculated diffraction patterns for $Sm_2Cu_{0.8}Pd_{0.2}O_4$ are shown in Fig. 2. The inset shows an enlargement of a selected area of the diffraction patterns: the full width at half maximum, $\Delta 2\theta$, of the peaks in this region is about 0.087° and is close to the instrumental resolution of the diffractometer used. The x-ray data on this sample are typical of all the samples studied, and provide a general indication of sample quality. The unit-cell parameters and the cell volumes determined by the profile analysis are given in Table I. In this table we also provide the ratio r_R/r_M in R_2MO_4 calculated according to Shannon;[28] r_M is the concentration-weighted mean radius of the four-coordinate cation. The c/a ratio is plotted in Figs. 3 and 4 as function of

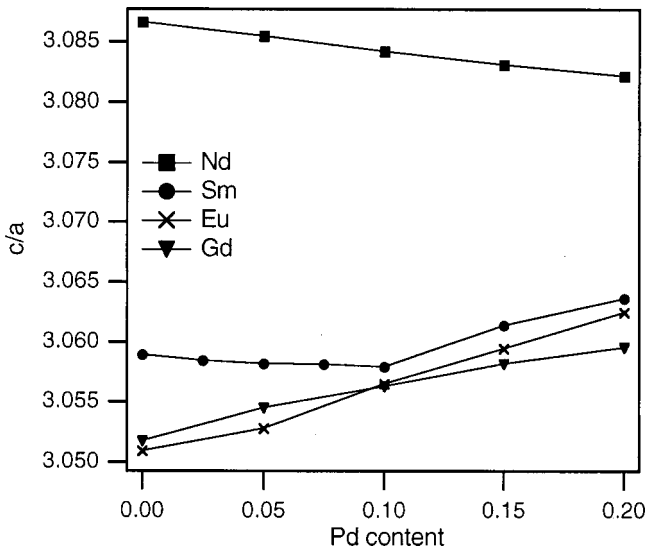

FIG. 3. c/a at room temperature as a function of palladium content for $R_2Cu_{1-x}Pd_xO_4$ with R=Nd, Sm, Eu, Gd, and $0 \leqslant x \leqslant 0.20$.

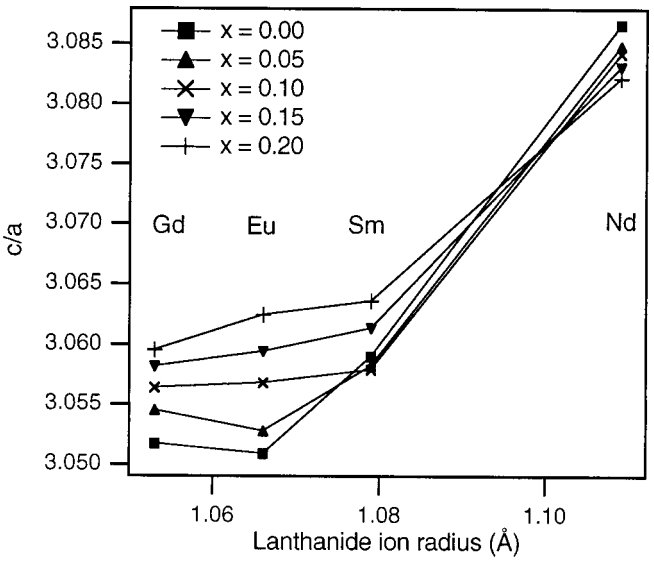

FIG. 4. c/a at room temperature as a function of the lanthanide radius for $R_2Cu_{1-x}Pd_xO_4$ with R=Nd, Sm, Eu, Gd and $0 \leqslant x \leqslant 0.20$.

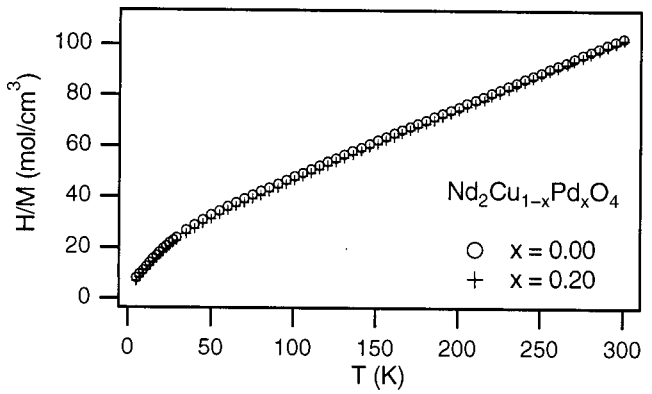

FIG. 5. Inverse molar susceptibility (FC) of $Nd_2Cu_{1-x}Pd_xO_4$ $x=0.0$, 0.2 measured in a field of 1 kG.

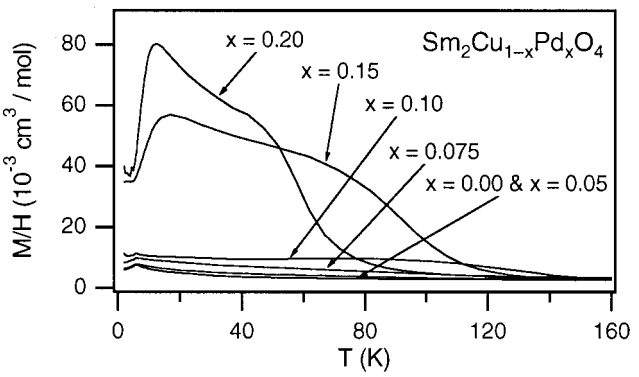

FIG. 6. FC molar susceptibility of $Sm_2Cu_{1-x}Pd_xO_4$ $0 \leqslant x \leqslant 0.20$ measured in a field of 100 G.

Pd content and lanthanide ionic radius,[28] respectively. The error bars are smaller than the markers. The individual unit-cell parameters and the cell volume increase smoothly with increasing Pd content and increasing lanthanide ionic radius as might be expected. However the c/a ratio decreases with increasing Pd content for Nd, but increases for Eu and Gd. The c/a ratio of the Sm-containing compounds shows a minimum at $x \sim 0.1$, where $r_R/r_M = 1.87$, the same value as calculated for Eu_2CuO_4. Furthermore, the c/a ratio of the Nd-containing compounds is about 1% larger than those of the other compounds, which have very similar c/a ratios, especially for $x \geqslant 0.1$.

Magnetometry

The inverse molar magnetic susceptibility (defined throughout this paper as H/M) of $Nd_2Cu_{1-x}Pd_xO_4$ ($x=0.0$, 0.2, FC) as measured in a field of 1 kG, is depicted in Fig. 5. The ZFC and FC data overlie for these compounds and also for $Nd_2Cu_{0.9}Pd_{0.1}O_4$ (not shown) and no field dependence was observed between these data and those measured in a field of 100 G. The data on Nd_2CuO_4 are in excellent agreement with those reported earlier.[14,18] We shall assume that the Cu^{2+} cations are antiferromagnetically coupled and do not contribute to the paramagnetic susceptibility, and that the temperature dependence seen in Fig. 5 is therefore due only to the Nd^{3+} cations. Fitting the high-temperature region ($T \geqslant 150$ K) to the Curie-Weiss law then results in an effective moment of 3.83, 3.83, and $3.80\mu_B/Nd^{3+}$ for $x=0.0$, 0.1, and 0.2 respectively. These values are in excellent agreement with values reported earlier.[17,18] The Weiss temperature is in all cases ~ -75 K, indicating the presence of some antiferromagnetic coupling. Below ~ 50 K the susceptibilities are higher than expected on the basis of the Curie-Weiss model, an observation which is in agreement with the data presented by Seaman.[14]

The FC susceptibility of $Sm_2Cu_{1-x}PdO_4$ ($x=0.0$, 0.05, 0.075, 0.10, 0.15, 0.2), measured in a field of 100 G, is plotted in Fig. 6, and in Fig. 7 a comparison between the low-temperature ZFC and FC data of $Sm_2Cu_{1-x}PdO_4$ ($x=0.0$, 0.2) is presented. Once again, the data on the composition $x=0.0$ are in good agreement with those published previously.[17] In general, the data in Figs. 6 and 7 show more features than those collected on the Nd analogs and, in order to facilitate a comparison between the various compositions, we shall use a number of characteristic temperatures T_n, which are listed in Table II, indicated in Fig. 7, and will be defined below. The compounds with $x \leqslant 0.10$ show a clear maximum in both ZFC and FC curves at ~ 6 K (T_1) but for larger values of x ($\geqslant 0.15$), a minimum is observed around this temperature. Simultaneously, a new maximum appears in the FC data at a temperature of between 12 and 17 K in 100 G (T_2). In the case of $x=0.15$ this maximum is broad, whereas for $x=0.20$ the peak is somewhat sharper. The maximum FC magnetization increases markedly with increasing Pd content, especially for $x \geqslant 0.15$. The inflection point in the FC data (T_3) is determined by the minimum in $d\chi/dT$ and T_4 is defined as the temperature above which the hysteresis between ZFC and FC data is not detectable in a field of 100 G. Similar characteristic temperatures in the Eu and Gd containing compounds will be labeled in an analogous fashion, although T_3 is not always lower than T_4. Figure 8 shows hysteresis loops for $Sm_2Cu_{0.8}Pd_{0.2}O_4$ at 5, 8, 30,

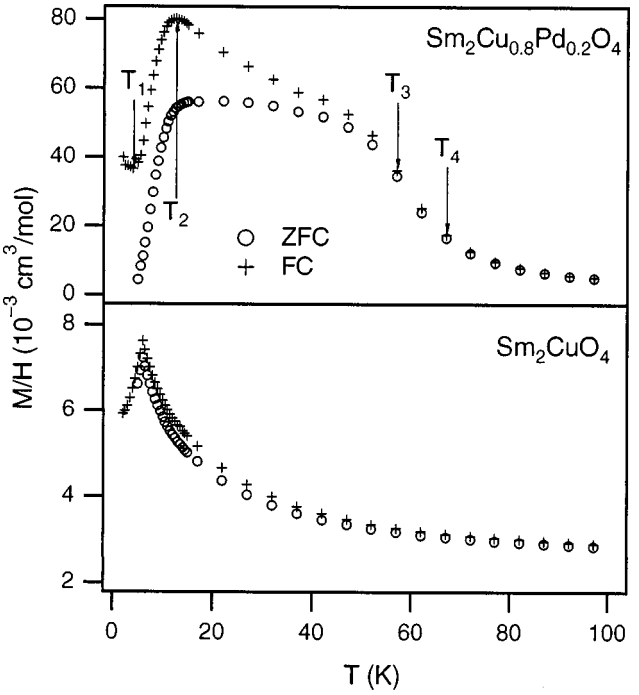

FIG. 7. Low-temperature molar susceptibility of $Sm_2Cu_{1-x}Pd_xO_4$ for $x=0.00$ (bottom) and $x=0.20$ (top) measured in a field of 100 G.

TABLE II. Signature temperatures (K) for $Sm_2Cu_{1-x}Pd_xO_4$ as measured in a field of 100 G. T_n are defined in the text and in Fig. 7. T_1, T_2 measured to ± 0.3 K.

x	T_1	T_2	T_3	T_4
0.0	6			200
0.05	6			180
0.075	6		117	138
0.10	6		112	127
0.15	5	17	92	107
0.20	5	12.5	57	62

70, and 200 K. On cooling from 200 to 70 K (i.e., $T > T_4$) a clear departure from linear behavior is observed and on cooling to 30 K, hysteresis becomes a dominant feature. However, the center of the hysteresis loop is not displaced from the origin, and there is no difference between ZFC (not shown) and FC hysteresis loops. At 8 K (i.e., $T \leqslant T_2$ in small fields), the remanant magnetization is very similar to that observed at 30 K, but the loop only closes at much higher fields: ~1800 G (8 K) vs ~800 G (30 K). At the lowest temperature measured (5 K) the center of the hysteresis loop is clearly shifted, and the loop does not close in the experimental field range. Displaced hysteresis loops (not shown) were also observed for $x = 0.05$, 0.10 at 5 K. As our initial measurements on $Sm_2Cu_{0.8}Pd_{0.2}O_4$ indicated a field dependence for T_2, we measured the FC magnetization of this sample in the temperature range $4.5 \leqslant T/\mathrm{K} \leqslant 15$, and the field range 10 G $\leqslant H \leqslant$ 50 kG. For $H \leqslant 100$ G, T_2 is constant at a value of 12.5 K; with increasing field it decreases until it reaches a minimum of 5.5 K in $H \geqslant 5$ kG.

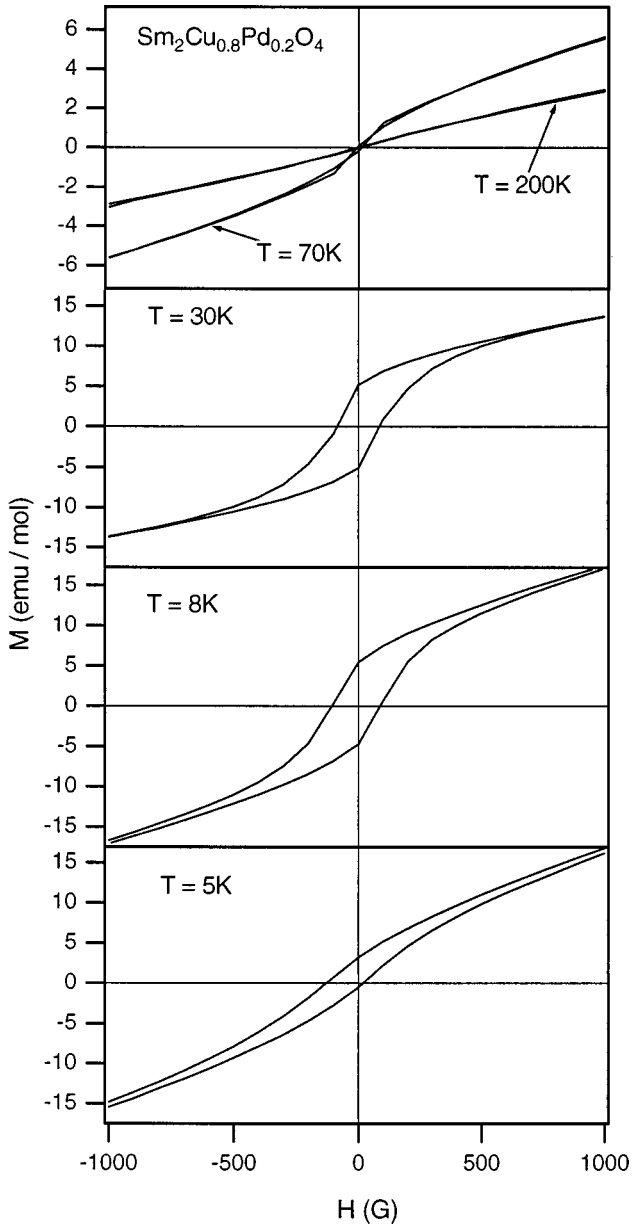

FIG. 8. Central portion of M:H for $Sm_2Cu_{0.8}Pd_{0.2}O_4$ at 5, 8, 30, 70, and 200 K after cooling from 300 K in a 2 kG field.

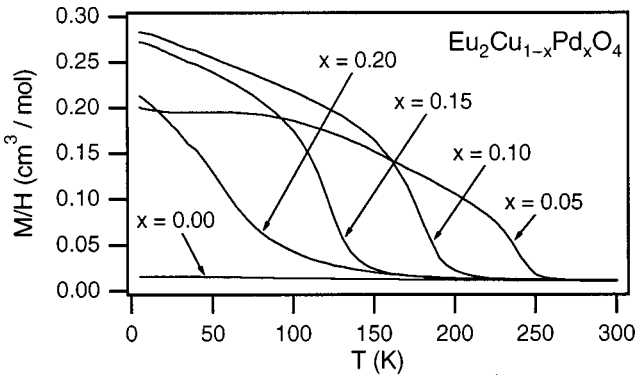

FIG. 9. FC molar susceptibility of $Eu_2Cu_{1-x}Pd_xO_4$, $0 \leqslant x \leqslant 0.20$, measured in a field of 100 G.

The FC magnetization of the compounds $Eu_2Cu_{1-x}Pd_xO_4$ as measured in a field of 100 G is presented as a function of temperature in Fig. 9. The europium containing compounds provide a useful comparison with the samarium and gadolinium compounds because of the nonmagnetic ground state of Eu^{3+}. Our data on Eu_2CuO_4 are in agreement with the data provided in Ref. 18, but are significantly different from those reported in Ref. 14. The compounds $Eu_2Cu_{1-x}Pd_xO_4$ with $x \geqslant 0.05$ show an inflection in the magnetization analogous to that seen at T_3 in the Pd-rich samarium compounds. On increased doping with Pd, T_3 decreases (Table III), while the maximum magnetization reaches a similar value for all compositions with $x \geqslant 0.05$ and this value is approximately an order of magnitude larger than measured for Eu_2CuO_4. Below T_4 hysteresis is observed in a field of 100 G for all compositions studied. This is exemplified for the Pd-doped samples by the FC hysteresis loops of $Eu_2Cu_{0.9}Pd_{0.1}O_4$ (Fig.

TABLE III. T_3 and T_4 (K) for $R_2Cu_{1-x}Pd_xO_4$ in a field of 100 G.

	Sm		Eu		Gd	
x	T_3	T_4	T_3	T_4	T_3	T_4
0.00		200		190	310	200
0.05		180	240	160	235	200
0.10	112	127	175	60	180	125
0.15	92	107	120	85	125	85
0.20	57	62	55	60	75	75

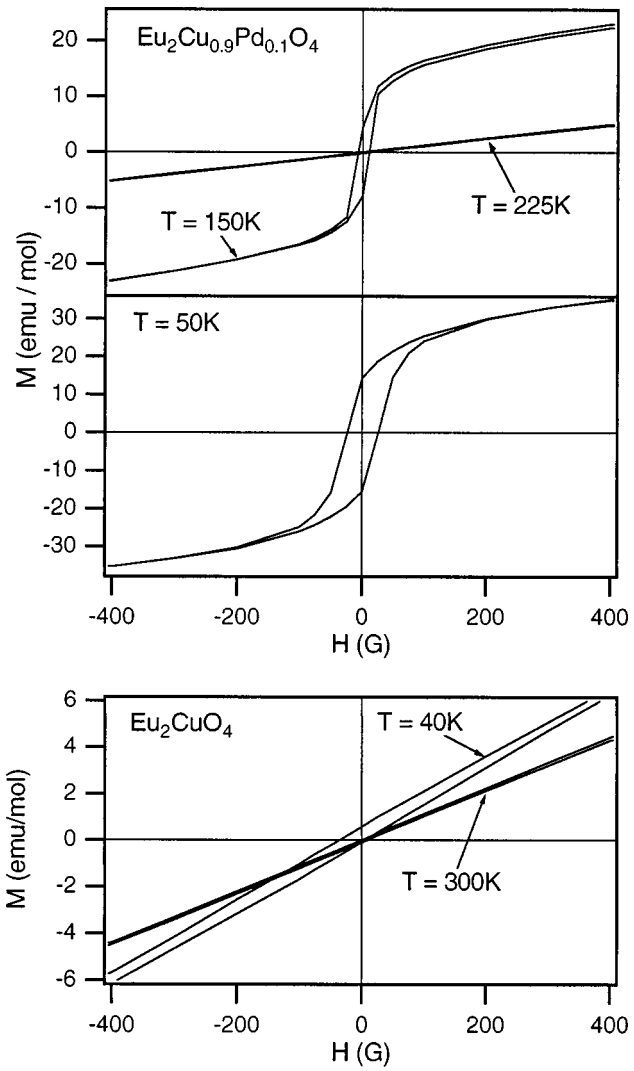

FIG. 10. Central portion of $M:H$ for $Eu_2Cu_{0.9}Pd_{0.1}O_4$ at 50, 150, and 225 K (top) and Eu_2CuO_4 at 300 and 40 K (bottom) after cooling from 300 K in a 2 kG field.

10). A linear M:H relationship is observed at temperatures higher than 225 K ($T>T_3$). On cooling below T_3 (to 150 K), the function becomes sigmoidal with a small amount of hysteresis apparent. Only at 50 K, that is below T_4, does hysteresis centered around the origin become a dominant feature. In contrast to the Pd-doped samples, the center of the hysteresis loop recorded at 40 K for Eu_2CuO_4 is displaced from the origin (Fig. 10).

The FC susceptibilities of $Gd_2Cu_{1-x}Pd_xO_4$ measured in a field of 100 G are presented in Fig. 11. All the Gd-containing compounds show an inflection in the measured susceptibility, similar to that observed at T_3 in the Sm samples, and the appearance of hysteresis below T_4. The values for T_3 and T_4 for the Gd-containing compounds are listed in Table III. The transition at T_3 has been linked to the appearance of a weak ferromagnetic (WFM) state.[14,21,31] However, the transition temperature we observe for Gd_2CuO_4 ($T_3\sim310$ K) is significantly higher than those reported before (~260 K). The presence of a WFM state in our sample at 300 K was confirmed by the nonlinear field dependence of the magnetization. The values of T_3 and T_4 decrease on increasing the amount of Pd substitution. The FC hysteresis loops on

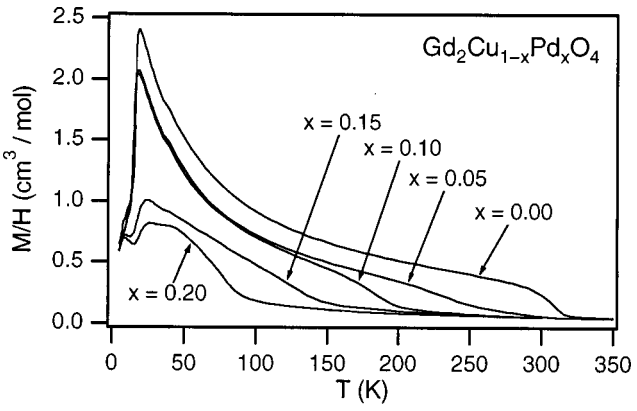

FIG. 11. FC molar susceptibility of $Gd_2Cu_{1-x}Pd_xO_4$, $0\leqslant x\leqslant0.20$, measured in a field of 100 G.

$Gd_2Cu_{0.9}Pd_{0.1}O_4$ (Fig. 12) show a linear field dependence at 300 K; a field dependence with a limited amount of hysteresis at 175 K ($T_3<T/\mathrm{K}<T_4$), and an increased hysteresis at lower temperatures (18 K), rather similar to the behavior of $Eu_2Cu_{0.9}Pd_{0.1}O_4$. On further cooling (to 5 K) the center of the hysteresis loop moves away from the origin.

DISCUSSION

Crystallographic characterisation

The results described above show that up to 20% of the Cu^{2+} cations in the T' compounds R_2CuO_4 can be replaced by the larger Pd^{2+} cation. Although we were able to refine all our x-ray data using the tetragonal space group $I4/mmm$, a previous single-crystal neutron-diffraction study[22] has shown that Gd_2CuO_4 is reduced to orthorhombic symmetry at room temperature by the rotation of the CuO_4 squares within the structure. It is not surprising that our analysis of x-ray powder-diffraction data did not reveal the displacements of the weakly scatterering oxide ions, but it does raise doubts about our space-group assignment in a number of other cases, although neutron diffraction has confirmed the undistorted structure of both Nd_2CuO_4 and Sm_2CuO_4.[9,15,16] In view of these uncertainties, we have examined our data in order to identify any indirect evidence of structural distortion. It has previously been assumed[23] that distortion occurs when the radius of R is lower than a critical value, but, in view of the nature of the solid solutions we are dealing with, we prefer to consider our data in terms of the radius ratio r_R/r_M (Table I). Given that Sm_2CuO_4 and Gd_2CuO_4 are, respectively, tetragonal and orthorhombic, we can assume that the critical radius ratio lies in the range $1.847<r_R/r_M<1.893$. Furthermore, Raman spectroscopy[32] has indicated that Eu_2CuO_4 is very close to the edge of the tetragonal stability field, and we therefore expect the critical radius ratio to be ~1.87. We thus expect, in the light of the results presented above, that $Sm_2Cu_{0.9}Pd_{0.1}O_4$ also lies on the edge of the stability field. The replacement of Cu^{2+} with Pd^{2+} decreases the ratio r_R/r_M, that is, the effective size of R is decreased and the degree of distortion is expected to increase. It has also been observed that, as a consequence of the rotation of the CuO_4 squares (Fig. 1), the ratio of the unit-cell parameters, c/a, is enhanced in the ortho-

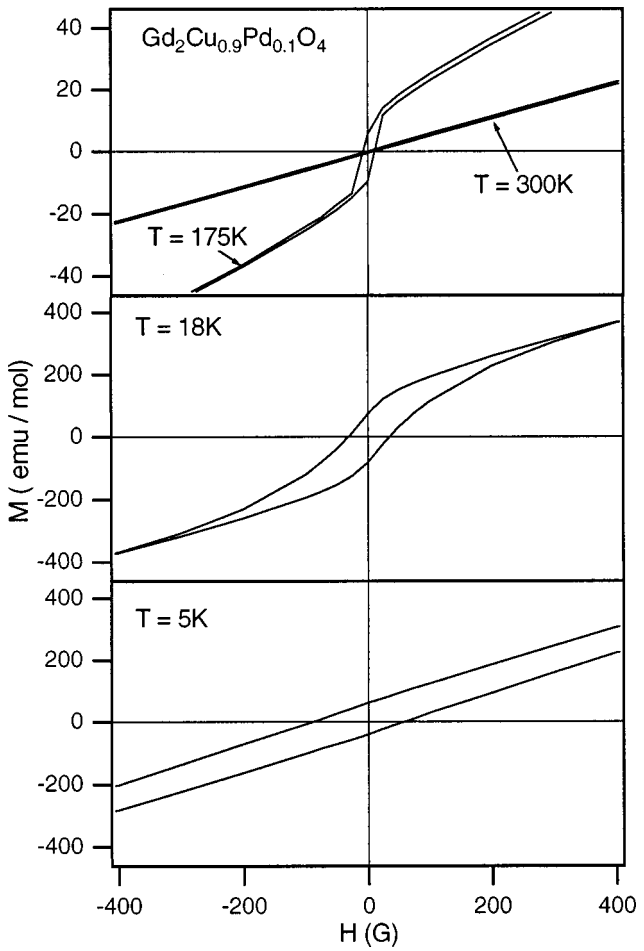

FIG. 12. Central portion of M:H for $Gd_2Cu_{0.9}Pd_{0.1}O_4$ at 5, 18, 225, and 300 K after cooling from 300 K in a 2 kG field.

rhombic phases of Gd_2CuO_4,[23] and also in $(Nd_{1-z}Tb_z)_{1.85}Ce_{0.15}CuO_4$.[33] We would therefore expect an increase in Pd content (x) to cause an enhancement of c/a in orthorhombic samples of $R_2Cu_{1-x}Pd_xO_4$, and we hypothesize that compositions having $r_R/r_M > 1.87$ and $\partial(c/a)/\partial x < 0$ are tetragonal, but that those having $r_R/r_M < 1.87$ and $\partial(c/a)/\partial x > 0$ are orthorhombic. Consideration of existing data on Gd_2CuO_4 and the data in Table I and Figs. 3 and 4 then leads us to conclude that all our Nd-containing samples are tetragonal, but that an orthorhombic distortion is introduced into the room-temperature structure of $Sm_2Cu_{1-x}Pd_xO_4$ within the composition range $0.075 \leqslant x \leqslant 0.1$, into $Eu_2Cu_{1-x}Pd_xO_4$ within the range $0 < x < 0.05$, and that it is present throughout the range $0 \leqslant x \leqslant 0.2$ for $Gd_2Cu_{1-x}Pd_xO_4$. We shall show below that this grouping is consistent with our magnetic data, in that these supposedly orthorhombic phases, and no others, show weak ferromagnetism below the ordering temperature of the Cu sublattice. The assumption that no further structural phase transitions occur below room temperature is consistent with our interpretation of the magnetic data, although it is not proven.

Magnetometry

Substitution of Cu by Pd in Nd_2CuO_4 has very little effect on the measured magnetic susceptibility (Fig. 5), thus emphasizing the extent to which the data are dominated by the contribution from the Nd^{3+} cations. The magnetic phase transitions affecting the Cu^{2+} sublattice, which have been seen only in neutron-diffraction experiments on undoped samples, are invisible in the susceptibilities of all our samples. We are, however, able to make two useful comments on the basis of these data. First, there is no evidence of weak ferromagnetism in the measured temperature range for any level of Pd doping, and secondly, the Nd sublattice does not order above 5 K. The former point is consistent with our suggestion that the Nd-containing compounds retain the tetragonal T' structure for all levels of Pd doping. The second may be due to the relatively large unit-cell parameters (and hence interatomic distances) in this system. Both of these observations are independent of our assumption that the Cu sublattice is antiferromagnetically ordered and does not contribute to the paramagnetic susceptibility. The marked dependence of the Néel temperature of the Cu sublattice on Pd concentration for $R = $ Sm, Eu, Gd, (to be discussed below) suggests that the Cu spins may be paramagnetic in our Nd samples at high temperature, and that the agreement between the observed and calculated effective magnetic moments may be due to the fact that the contribution from the Nd^{3+} cations is large enough to render that from Cu^{2+} insignificant.

The lack of change in the susceptibility of the Nd compounds on doping is in marked contrast to the behavior of the compounds containing smaller rare earths. The magnetic behavior of Sm_2CuO_4 can be interpreted in terms of an antiferromagnetic Cu sublattice and a Sm sublattice which orders antiferromagnetically at $T_1 = 6$ K. The latter transition is apparent in our data (Fig. 6), although the former is not and we must again base our interpretation on previous neutron studies. On doping with Pd, very little change in susceptibility is apparent for $x \leqslant 0.075$, with the Néel temperature of the Cu sublattice remaining invisible and the antiferromagnetic transition on the Sm lattice being retained. However, a small susceptibility enhancement is apparent at ~ 140 K for $x = 0.10$, and more marked enhancements are present for $x = 0.15$ and 0.20, albeit with lower onset temperatures (~ 130 and 90 K, respectively). We believe that these features are associated with a weakly ferromagnetic ordering of the Cu^{2+} cations. They occur at temperatures much lower than the Néel temperature of Sm_2CuO_4 as a consequence of the dilution of the Cu sublattice by diamagnetic Pd^{2+}. The weak ferromagnetic component is allowed by the reduction in symmetry which accompanies the introduction of $\geqslant 10\%$ Pd. The temperatures quoted above were determined by inspection of the data in Fig. 6, and are all somewhat higher than the more strictly defined values of T_3 listed in Table II. This difference is a consequence of the relatively broad transitions observed in these disordered materials; using our data it is impossible to identify precisely the temperature at which long-range magnetic ordering is established. Hysteresis between FC and ZFC susceptibilities is apparent at low temperatures ($< T_4$) in all the Sm containing compounds. This is not surprising in the case of those which are weakly ferromagnetic, and in the case of those having $0 < x < 0.10$ it could be explained by invoking the presence of frozen decoupled spins on the diluted Cu sublattice. However, this does not explain why a very small amount of hysteresis is apparent below 50 K in undoped Sm_2CuO_4 (Fig. 7). For all

the tetragonal samples ($0<x<0.1$), the hysteresis may be a consequence of frustration on the Cu sublattice of the undistorted unit cell. We shall return to this point below. The behavior of the Pd-doped samples at temperatures lower than 40 K is complex and, for $x>0.1$, it bears a strong resemblance to that of orthorhombic Gd_2CuO_4. Increasing the Pd content converts the maximum at ~6 K into a minimum, but creates a broader maximum at T_2. However, the value of T_2 is field dependent, and for fields in excess of 5 kG, $T_2=6$ K. We believe that the maximum at T_2, which becomes more pronounced with increasing Pd content, is not a true phase transition, but is a consequence of the magnetic moments of the Sm cations aligning with the net magnetic moment of the Cu sublattice. This is consistent with the obvious nature of the maximum at T_2 for $x>0.1$, when weak ferromagnetism is clearly present, although it is impossible to identify T_2 in the sample $x=0.1$, which is a weak ferromagnet with a smaller net moment. We suggest that the degree of alignment increases with the strength of the field, but that alignment is opposed by the tendency of the Sm sublattice to show short-range antiferromagnetic order when the temperature is only slightly higher than the Néel temperature (T_1) of that sublattice. Consequently, in a relatively high field the Sm-Cu alignment is established immediately at the temperature at which long-range ordering of the Sm spins is lost ($T_2=T_1$), whereas in a lower field the short-range Sm-Sm interactions prevent the maximum magnetization being achieved until a slightly higher temperature ($T_2>T_1$). The origin of the increase in susceptibility which occurs below 6 K in the more heavily doped samples is not clear, although the displaced hysteresis loop recorded for $Sm_2Cu_{0.8}Pd_{0.2}O_4$ at 5 K (Fig. 8) suggests that a degree of spin frustration is present in this temperature region. The other hysteresis loops drawn in Fig. 8 are consistent with a description in which at 200 K the Sm and Cu spins are all paramagnetic. At 70 K nonlinear $M:H$ behavior is apparent, and in the range $8 \leqslant T/\mathrm{K} \leqslant 30$ the sample shows hysteresis behavior characteristic of a weak ferromagnet.

The description of $Sm_2Cu_{1-x}Pd_xO_4$ given above is consistent with data collected on $Eu_2Cu_{1-x}Pd_xO_4$ in that the latter can be interpreted as showing the onset of ordering on the Cu sublattice, with a weak ferromagnetic component, at temperatures which decrease from 260 K for $x=0.05$ to ~190 K for $x=0.20$. Once again, these temperatures, estimated by inspection are higher than T_3 (Table III). The smaller size of Eu^{3+} compared to Sm^{3+} results in the orthorhombic phase being adopted at relatively low dopant levels, conveniently rendering visible the ordering of the Cu sublattice for all samples other than $x=0.0$. We believe that although the latter composition may lie very close to the stability limit of the tetragonal phase, the contrast between the data for $x=0.0$ and $x=0.05$ provides convincing evidence that the end member does adopt an undistorted T' structure. The increase in the magnetic ordering temperature on moving from Sm to Eu at constant Pd content can be ascribed to the decrease in interatomic distances which results from the reduction in unit-cell volume. However, this explanation ignores the increase in the rotation of the CuO_4 squares that would be expected to accompany the change from Sm to Eu. The proposal that the complex behavior observed below 30 K for $R=$Sm is a consequence of magnetic Cu-Sm interactions is consistent with the absence of such behavior when $R=$Eu, that is a cation with a diamagnetic ground state. The hysteresis loops plotted in Fig. 10 for $Eu_2Cu_{0.9}Pd_{0.1}O_4$ are symmetrical about the origin, and they are therefore consistent with the presence of weak ferromagnetism; there is no evidence of frustration or spin-glass behavior in this composition. The maximum net magnetic moment increases with Pd content in the range $0<x<0.1$, taking a value, for $x=0.1$, of 5×10^{-3} μ_B per formula unit in 100 G, increasing to 8.5×10^{-3} μ_B in 1 kG. Further doping ($x>0.1$) leads to a decrease in this value, presumably because the magnetic dilution of the four-coordinate sublattice outweighs the effect of the crystallographic distortion which permits the weak ferromagnetism. The low-temperature behavior of undoped Eu_2CuO_4 is noteworthy. The observation of a displaced hysteresis loop having a significant width indicates that a spin-glass-like state is present in the Pd-free tetragonal phase at 40 K, and, in view of the nonmagnetic nature of the Eu^{3+} cation, it must be associated with the Cu sublattice, as tentatively proposed above for the case of $R=$Sm, $x<0.10$. This leads us to suggest that the frustration on the Cu^{2+} sublattice can lead to re-entrant spin-glass behavior in tetragonal T'-phases, although further experimental work is needed in order to validate this hypothesis.

The last series of compounds to discuss is $Gd_2Cu_{1-x}Pd_xO_4$, the end member ($x=0.0$) of which is known[22] to be orthorhombic at room temperature. Our data indicate a somewhat higher magnetic ordering temperature (310 K) than has been reported previously (~260 K) for this composition. We believe that this discrepancy is due to the experimental procedure used to measure the variation of magnetization with temperature. The data on $Gd_2Cu_{1-x}Pd_xO_4$ ($x=0.0,0.05$) shown in Fig. 11 were collected after field cooling from 350 K. Our preliminary studies, in which the Gd_2CuO_4 was cooled from 300 K, showed a transition temperature close to the literature value; we believe that unwitting failure to warm the sample above the Curie temperature has previously lead to an incorrect result. A hysteresis loop taken at 350 K showed a linear dependence of $M:H$, whereas nonlinearity was apparent at 300 K. The trends established by the comparison of samples containing Sm and Eu are maintained by the Gd-containing phases. The further reduction in the ratio r_R/r_M ensures weak ferromagnetism in all compositions, with the ordering temperature of the Cu sublattice visibly (Fig. 11) decreasing as the degree of dilution by Pd increases. The complex low-temperature behavior resembles that seen in the Sm system but not in the Eu system, thus providing further evidence that it involves interactions between the ordered Cu sublattice and paramagnetic lanthanide cations. However, the relative size of the maximum at T_2 decreases with x in the case of Gd, in contrast to the composition dependence observed for $R=$Sm. The illustrative hysteresis loops shown in Fig. 12 confirm the presence of a spontaneous magnetization in $Gd_2Cu_{0.9}Pd_{0.1}O_4$. There is some indication of a displacement in the hysteresis loop collected at 5 K, which is below the ordering temperature of the Gd sublattice, but it is not as marked as that seen (Fig. 8) in the case of $Sm_2Cu_{0.8}Pd_{0.2}O_4$.

CONCLUSIONS

We have presented evidence which supports previous claims that weak ferromagnetism is observed in T' cuprates

which have undergone a phase transition to orthorhombic symmetry. We have shown that the occurence of such a transition does not depend on the chemical character of the lanthanide (or lanthanides) in the sample, nor simply on the size of the lanthanide cation, but on the ratio of the mean size of the lanthanide to the mean size of the transition-metal cation occupying the four-coordinate site. The critical value of r_R/r_M below which the orthorhombic phase is stable has been shown to lie close to 1.87. It is possible to introduce weak ferromagnetism into T' systems which contain only one relatively large lanthanide, for example Sm^{3+}, by controlling chemically the size of the transition-metal site, that is, ferromagnetism can be induced in an antiferromagnetic cuprate by substituting a diamagnetic cation on the Cu sublattice. However, there are some lanthanides, for example Nd^{3+}, which are too large for this strategy to be successful within the composition range studied. The low-temperature magnetic behavior of these compounds is complex, and involves both R-R and R-Cu interactions. There is evidence to suggest that a re-entrant spin glass forms on the Cu sublattice of tetragonal T' structures, for example Eu_2CuO_4, at low temperatures. We have also seen behavior suggestive of the presence of a spin-glass component at 5 K in orthorhombic Sm-containing samples. The origin of this latter behavior is not clear.

ACKNOWLEDGMENTS

We are grateful to EPSRC for financial support, and to A. J. Tomlinson and P. H. Munns for experimental assistance.

*Author to whom correspondence should be addressed.

[1] J. G. Bednorz and K. A. Muller, Z. Phys. B **64**, 189 (1986).
[2] H. Müller-Buschbaum and W. Wollschläger, Z. Anorg. Allg. Chem. **414**, 76 (1975).
[3] Y. Tokura, H. Takagi, and S. Uchida, Nature (London) **337**, 345 (1989).
[4] H. Takagi, S. Uchida, and Y. Tokura, Phys. Rev. Lett. **62**, 1197 (1989).
[5] G. M. Luke, B. J. Sternlieb, Y. J. Uemura, J. H. Brewer, R. Kadono, R. F. Kiefl, S. R. Kreitzmann, T. M. Riseman, J. Gopalakrishnan, A. W. Sleight, M. A. Subramanian, S. Uchida, H. Takagi, and Y. Tokura, Nature (London) **338**, 49 (1989).
[6] J. W. Lynn, I. W. Sumarlin, S. Skanthakumar, W.-H. Li, R. N. Shelton, J. L. Peng, Z. Fisk, and S.-W. Cheong, Phys. Rev. B **41**, 2569 (1990).
[7] P. Bourges, L. Boudarène, and D. Petitgrand, Physica B **180 & 181**, 128 (1992).
[8] Y. Endoh, M. Matsuda, K. Yamada, K. Kakurai, Y. Hidaka, G. Shirane, and R. J. Birgeneau, Phys. Rev. B **40**, 7023 (1989).
[9] M. Matsuda, K. Yamada, K. Kakurai, H. Kadowaki, T. R. Thurston, Y. Endoh, Y. Hidaka, R. J. Birgeneau, M. A. Kastner, P. M. Gehring, A. H. Moudden, and G. Shirane, Phys. Rev. B **42**, 10 098 (1990).
[10] D. Petitgrand, L. Boudarène, P. Bourges, and P. Galez, J. Magn. Magn. Mater. **104–107**, 585 (1992).
[11] G. Aeppli and D. J. Butterey, Phys. Rev. Lett. **61**, 203 (1988).
[12] D. Vaknin, S. K. Sinha, D. E. Moncton, D. C. Johnston, J. M. Newsam, C. R. Safinya, and H. E. King, Phys. Rev. Lett. **58**, 2802 (1987).
[13] M. J. Rosseinsky, K. Prassides, and P. Day, Chem. Commun. (London), 1734 (1989).
[14] C. L. Seaman, N. Y. Ayoub, T. Bjørnholm, E. A. Early, S. Ghamaty, B. W. Lee, J. T. Markert, J. J. Neumeier, P. K. Tsai, and M. B. Maple, Physica C **159**, 391 (1989).
[15] A. G. Gukasov, V. A. Polyakov, I. A. Zobkalo, D. Petitgrand, P. Bourges, L. Boudarène, S. N. Barilo, and D. N. Zhigunov, Solid State Commun. **95**, 533 (1995).
[16] I. W. Sumarlin, S. Skanthakumar, J. W. Lynn, J. L. Peng, Z. Y. Li, W. Liang, and R. L. Greene, Phys. Rev. Lett. **68**, 2228 (1992).
[17] M. F. Hundley, J. D. Thompson, S.-W. Cheong, Z. Fisk, and S. B. Oseroff, Physica C **158**, 102 (1989).
[18] R. Saez-Puche, M. Norton, T. R. White, and W. S. Glaunsinger, J. Solid State Chem. **50**, 281 (1983).
[19] A. D. Alvarenga, D. Rao, J. A. Sanjurjo, E. Granado, I. Tooriani, C. Rettori, S. Oseroff, J. Sarrao, and Z. Fisk, Phys. Rev. B **53**, 837 (1996).
[20] A. G. Gukasov, S. Y. Kokovin, V. P. Plakhty, I. A. Zobkalo, S. N. Barilo, and D. I. Zhigunov, Physica B **180–181**, 455 (1992).
[21] J. D. Thompson, S.-W. Cheong, S. E. Brown, Z. Fisk, S. B. Oseroff, M. Tovar, D. C. Vier, and S. Schultz, Phys. Rev. B **39**, 6660 (1989).
[22] M. Braden, W. Paulus, A. Cousson, P. Vigoureux, G. Heder, A. Goukassov, P. Bourges, and D. Petitgrand, Europhys. Lett. **25**, 635 (1994).
[23] P. Vigoureux, M. Braden, A. Gukasov, W. Paulus, P. Bourges, A. Cousson, D. Petitgrand, J. P. Lauriat, M. Neven, S. N. Barilo, D. I. Zhigunov, P. Adelmann, and C. Heger, Physica C **273**, 239 (1997).
[24] A. Butera, M. Tovar, S. B. Overoff, and S. Fisk, Phys. Rev. B **52**, 13 444 (1995).
[25] M. Tovar, X. Obradors, F. Pérez, S. B. Oseroff, R. J. Duro, J. Rivas, D. Chateigner, P. Bordet, and J. Chenavas, Phys. Rev. B **45**, 4729 (1992).
[26] S. B. Oseroff, D. Rao, F. Wright, D. C. Vier, S. Schultz, J. D. Thompson, Z. Fisk, S.-W. Cheong, M. F. Hundley, and M. Tovar, Phys. Rev. B **41**, 1934 (1990).
[27] L. B. Steren, M. Tovar, and S. B. Oseroff, Phys. Rev. B **46**, 2874 (1992).
[28] R. D. Shannon, Acta Crystallogr. Sect. A: Cryst. Phys., Diffr., Theor. Gen. Crystallogr. **32**, 519 (1976).
[29] H. M. Rietveld, J. Appl. Crystallogr. **2**, 65 (1969).
[30] A. C. Larson and R. B. von-Dreele, General Structure Analysis System (GSAS), Los Alamos National Laboratories, 1990.
[31] H. D. Yang, T. H. Meen, and Y. C. Chen, Phys. Rev. B **48**, 7720 (1993).
[32] M. A. Laguna, M. L. Sanjuán, A. Butera, M. Tovar, Z. Fisk, and P. Canfield, Phys. Rev. B **48**, 7565 (1993).
[33] M. Braden, P. Adelmann, P. Schweiss, and T. Woisczyk, Phys. Rev. B **53**, R2975 (1996).